Optical and thermal performances of a solar parabolic trough collector under climate conditions of the Cameroon Sahelian Zones

Joseph Kessel Pombe[1-2], Haman-Djalo[3], Beda Tibi[3], Etienne Tchoffo Houdji[4], and Steven Heugang Ndjanda[4]

[1]Faculty of Sciences, Department of Physics, The University of Maroua, P.O. Box 814, Cameroon

[2]Department of Applied Sciences, Université du Québec en Abitibi-Temiscamingue,
445 Boulevard de l'Université, Rouyn-Noranda, QC J9X 5E4, Canada

[3]Faculty of Sciences, Department of Physics, The University of Ngaoundere, P.O. Box 405, Cameroon

[4]The Higher Institute of the Sahel, Department of Renewables Energy, The University of Maroua, P.O. Box 46, Cameroon

ABSTRACT: Detailed simulations in aim to evaluated performances of a solar parabolic trough collector under climatic conditions of Cameroon Sahelian Zones was devoted by using a computer program based on one-dimensional flow implicit finite volume method with energy balance. The heat collecting element of the collector was divided into several control volume and heat balance correlations was applied for each control volume of the trough. In other to solve the three linear algebraic equations obtained from the model, the Tri-Diagonal Matrix Algorithm was implemented. At all, the model estimates for a typical day of the least sunny and the sunniest months, the optical and thermal performances of the collector, the solar energy absorbed the useful thermal heat and the heat lost to the ambient. The E-W horizontal traking mode which is getting closer with full tracking mode is assumed to collect high optical efficiency at about 74% during all the seasons. The maximum of outlet temperature of heat transfer fluid obtained at the right end of the absorber tube is about 140°C, 138°C and 80°C during a typical day of the least sunny months and 180°C, 180°C and 90°C during a typical day of the sunniest month respectively for water, air and TherminolVP-1[TM] synthetic oil used as heat transfer fluid. Outlet temperatures obtained from the model compared with data from Sandia experimental tested collector and from another devoted work show that the model is very suitable to predict the behavior of a solar parabolic trough collector under climatic conditions of Cameroon Sahelian Zones.

KEYWORDS: Simulation, finite volume method, tracking modes, Far North Cameroon Region.

1   INTRODUCTION

Solar energy is a very interesting alternative to meet Cameroon Sahelian Zones energy needs and solar parabolic trough collectors offer good solutions for a large scale harnessing of solar energy with about 3490 hour/year of sunshine duration in Far North Cameroon region. A solar parabolic trough collector uses reflectors to concentrate direct solar radiation into a heat collection element located along a small focal line of the parabola. Thus, the concentrated solar radiation is absorbed and converted into useful thermal energy through the heat transfer fluid flowing through the absorber tube. Once the physical characteristics and thermal properties of the heat transfer fluid are known, the optical and thermal performances and even energy gained by the heat transfer fluid can be calculated in other of such configurations and meteorological conditions. Thus, the outlet temperature of the heat transfer fluid and thermal efficiency obtained indicate clearly the thermal performances of the model.

Many studies have been carried out to analyze thermal and optical performances of solar parabolic trough collectors in different localities. Also many numerical method and software tools have been used and most of results from simulation devoted were validated with data from Sandia National Laboratories experimental tested collector. For example, Kalogirou Soteris A. [1] developed a model of solar parabolic trough collector and solved it by using Engineering Equation Solver in aim to analyze the performances of the collector installed in Cyprus University of Technology. The model was validated by results from Sandia National Laboratories experimental tested collectors. Ya-Ling. He, Jie. Xiao, Ze-Dong. Cheng, Yu-Bing. Tao [2] simulate the LS-2 solar collector by using a coupled method based on Monte Carlo Ray Trace (MCRT) and Finite Volume Method to solve the complex coupled heat transfer problem of radiation, heat conduction and convection. According to results, four outlet temperatures with good agreement were counted out and compared with Dudley, V. E., Kolb, G. J., Sloan, M., Kearney, D et al., [3] report data. Experimental data from Sandia National Laboratories experimental tested collector were used by A. A. Hachicha, I. Rodríguez, R. Capdevila and A. Oliva [4] to validate numerical heat transfer model of a solar parabolic trough collector based on the finite volume method. Results obtained show a good agreement with experimental data. By dividing into several segments a heat collection element of a solar parabolic trough collector and by applying heat transfer balance equations in each segment of the trough, Modified Euler Method were applied by Ouagued M, Khellaf A, Loukarfi L [5] to solve a system of differential equations that govern the heat balances in each segment in aim to analyze thermal performances of a parabolic trough collector under Algerian climate. Results indicated that with the increase in temperature of absorber tube and heat transfer fluid, the heat loss of the parabolic trough collector increases and also heat gain decreases. Mohanad Abdulazeez Abdulraheem Alfellag [6] applied mathematical model in aim to estimate thermal performances of a solar parabolic trough collector located at Embry-Riddle Aeronautical University, Daytona Beach. By dividing the model in three parts and implemented it into Matlab, results from simulation gives acceptable agreement with experimentation and indicated a maximum temperature of 48°C and a maximum efficiency of 30 % for water used as heat transfer fluid. To determine the performances and the outlet temperature of TherminolVP-1™ oil and liquid water used as heat transfer fluid in a solar parabolic trough collector in Algerian Saharan region climate conditions, Yacine Marif, Hocine Benmoussa, Hamza Bouguettaia, Mohamed M. Belhadj, Moussa Zerrouki [7] recently used one dimensional implicit finite difference numerical method. Results obtained were validated by data from Sandia National Laboratories experimental tested collectors and shown that the thermal efficiency was about 69.73–72.24%. More recently, Joseph Kessel Pombe, Camelia Stanciu, Haman-Djalo, Viorel Badescu and Beda Tibi [8] investigated energy balance of heat collection element of a solar parabolic trough collector by using air as heat transfer fluid. The model based on one-dimensional flow was solved by applying pdepe tool's Matlab to evaluate the maximum temperature of air obtained at the outlet of heat collection element at about 590 K and this was expected to study the performances and relevant areas pertaining of a solar parabolic trough collector in Sahelian zones.

Many researchers worked and analyzed performances of solar parabolic trough collectors in different localities and for several applications. Also many numerical method and heat balance correlations were used. In addition, geometrical and thermo physical characteristics were used in modeling and results from Sandia experimental tested collector were used to validate several numerical models. But none of them worked on optical and thermal performances of solar parabolic trough collectors in Sahelian climatic conditions. Furthermore, to date, no solar parabolic trough collector has been installed in Sahelian zones and particularly in Cameroon Sahelian Zones and none is under construction. Moreover, studies have been rarely conducted in order to evaluate solar direct radiation, solar parabolic trough collector performances and relevant areas pertaining. By highlighting some researchers work, this study aims at filling that gap by analyzing performances of solar parabolic trough collectors in climatic conditions of Cameroon Sahelian zones. Finite volume numerical method based one-dimension flow is used for modeling and computer program is used for implementation.

2 METHODOLOGY OF THE WORK

2.1 CHARACTERISTICS OF THE MODEL

We have used (Table 1) the geometrical and thermo-physical properties of the Sandia National Laboratory experimental tested collector installed in the Mojave Desert in South of California to analyse performances of a solar parabolic trough collector under climatic conditions of Cameroon Sahelian Zones.

Table 1. Geometrical and Thermo-physical Characteristics of the Solar Parabolic Trough Collector [9]

	Symbol	Physical parameters	Value	Unit
Collector	L	Length	7.8	m
	W	Aperture	5	m
	F	Focal length	1.840	m
Reflector	C_{refl}	Specific heat	581	J/kg K
	ρ_{refl}	Density	2400	kg/m^3
	e	Thickness	0.005	m
	α_0	Transmittance-absorptance factor	0.864	-
	ρ_0	Reflectivity	0.93	-
	γ	Shape factor	0.92	-
Glass envelope	dev	External diameter	0.115	m
	div	Internal diameter	0.112	m
	k_{gl}	Thermal conductivity	1.2	W/mK
	α_{ver}	Thermal absorptance	0.02	-
	C_{gl}	Specific heat	1090	J/kg K
	ρ_{gl}	Density	2230	kg/m^3
	ε_{gl}	Emissivity	0.86	-
	τ_{gl}	Transmittance	0.95	-
Absorber	dea	External diameter	0.070	m
	dia	Internal diameter	0.066	m
	k_{abs}	Thermal conductivity	54	W/mK
	α_{abs}	Thermal absorptance	0.906	-
	C_{pabs}	Specific heat	500	J/kg K
	ρ_{abs}	density	8020	kg/m^3
	ε_{abs}	Emissivity	0.14	-

2.2 SITE LOCATION

Cameroun Sahelian Zones include two Regions, North and Far North. The site location our study concerns is specifically Maroua which is located in the Far North Region of Cameroon. The characteristics of the site from Maroua Sallak weather Airport are given in Table 2.

Table 2. Geographical Coordinates of the Studied Location from Maroua Sallak weather Airport

Position studied	Latitude (°)	Longitude (°)	Altitude (m)	Climate	Albedo
Maroua	5.15	13.58	718	Tropical and Sahelian	0.6

2.3 SOLAR RADIATION MODEL

Sahelian Zones are known of an arid climate with irregular rainfall, low cloudiness of the atmosphere, hot and dry air, permanent aerosols, almost ten sunny months of dry seasons and two less sunny months of wet seasons. Under these climatic conditions, the empirical model of Capderou [10] based clear sky seems suitable to explore in order to estimate direct solar radiation received on a collector surface located in any Cameroon Sahelian Zones and even his optical efficiency.

2.3.1 ESTIMATION OF SOLAR DIRECT RADIATION ON A HORIZONTAL PLANE

The solar direct radiation on a horizontal plane is estimated as follow:

$$I_{dir}\left(W.m^{-2}\right) = I_0 \times \varepsilon_0 \times \cos(\theta) \times \exp\left(-T_L\left(0.9 + \frac{9.4}{(0.89)^z}\sinh_s\right)^{-1}\right) \tag{1}$$

In this study, the mean value of the solar constant flux received on the ground is assumed to be set:

$I_0 = 1367 \text{W.m}^{-2}$.

The correction coefficient of the Earth-Sun distance can be calculated by the equation (2):

$$\varepsilon_0 (-) = 1 + 0.034 \times \cos\left(\frac{360}{365}(n-2)\right) \tag{2}$$

Where n is the day number of the year, ranging from 1 on 1 January to 365 on 31st December.

In this work, we assume the solar tracking modes on one axis based the cosine of incidence angle $\cos(\theta)$ as well as proposed by Capderou [10] in Table 3:

Table 3.   Estimation of the Cosine of Incidence Angle Trough the Solar Tracking Mode

Tracking mode	Tubular receiver orientation	Cosine of incidence angle
East-West polar tracking	Along the earth axis	$\cos\theta = \cos\delta$
East-West horizontal tracking	Parallel to the North-South axis	$\cos\theta = \left(1 - \left(\cos(\delta)\sin(\varphi)\cos(\omega) - \sin(\delta)\cos(\varphi)\right)^2\right)^{\frac{1}{2}}$
North-South horizontal tracking	Parallel to the East-West axis	$\cos\theta = \left(1 - \cos^2(\delta)\sin^2(\omega)\right)^{\frac{1}{2}}$

The absorption and diffusion caused by the atmospheric constituents can be expressed by the Linke turbidity factor which is calculated based clear sky as given:

$$T_{Lf}(-) = T_0 + T_1 + T_2 \tag{3}$$

With

The modeling of the turbidity factor of gaseous absorption based only on geo-astronomical parameters is given by the following expression:

$$T_0(-) = (2.4 - 0.9\sin\varphi) + 0.1 \times Ah_e(2 + \sin\varphi) - 0.2z - (1.22 + 0.14 \times Ah_e)(1 - \sinh_s) \tag{4}$$

The turbidity factor of absorption by atmospheric gases (O_2, CO_2 and O_3) is calculated by the following formula:

$$T_1(-) = (0.89)^z \tag{5}$$

The turbidity factor caused by aerosols is calculated by the following formula:

$$T_2(-) = (0.9 + 0.4 \times Ah_e) \times (0.63)^z \tag{6}$$

With $z(m)$ is the altitude of the site location.

The parameter which characterize seasons is calculated as follow:

$$Ah_e(-) = \sin\left(\frac{360}{365}(n-121)\right) \tag{7}$$

The sun elevation angle is calculated as follow:

$$h_s(°) = \cos\varphi\cos\delta\cos\omega + \sin\varphi\sin\delta \tag{8}$$

2.3.2   ESTIMATION OF SOLAR DIFFUSE RADIATION ON A HORIZONTAL PLANE

The diffuse component of solar radiation received on a horizontal plane is given:

$$I_{dif}\left(W.m^{-2}\right) = I_0 \times \varepsilon_0 \times \exp\left(-1 + 1.06 \times \log\left(\sin(h_s)\right) + \xi\right) \tag{9}$$

With:

$$\xi = 1.1 - \sqrt{\left(\log(T_1 + T_2) - 2.8 + 1.02(1 - \sinh_s)^2\right)^2 + (1.1)^2} \tag{10}$$

2.3.3   ESTIMATION OF SOLAR GLOBAL RADIATION ON A HORIZONTAL PLANE

It is the sum of the direct and diffuse solar radiation given as follow:

$$G_{sol}\left(W.m^{-2}\right) = I_{dir} + I_{diff} \tag{11}$$

2.3.4   SOLAR ENERGY ABSORBED

For a solar parabolic trough collector, the incident solar radiation absorbed per unit of area by the absorber tube is given:

$$Q_{abs}\left(W\right) = A_0 \times I_{dir} \times \rho_0 \times \alpha_0 \times \gamma \times K \tag{12}$$

For a solar parabolic trough collector, the incident solar radiation absorbed per unit of area by the glass envelope is given:

$$Q_{ge}\left(W\right) = A_0 \times I_{dir} \times \rho_0 \times \alpha_{ge} \times \gamma \times K \tag{13}$$

The aperture area of a solar parabolic trough collector is calculated as follow:

$$A_0\left(m^2\right) = W \times L \tag{14}$$

The transmittance-absorptance factor is calculated in the following form:

$$\alpha_0\left(-\right) = \frac{\tau_{ge} \times \alpha_{abs}}{1 - (1 - \alpha_{abs})(1 - \tau_{ge})} \tag{15}$$

The shape factor is calculated as follow

$$\gamma\left(-\right) = \prod_{i=1}^{6} \gamma_i \tag{16}$$

The incident angle modifier is calculated:

$$K\left(-\right) = 1 - 0,00384\left(\theta\right) - 0,000143\left(\theta^2\right) \tag{17}$$

The solar parabolic trough collector optical efficiency is defined in the following form:

$$\eta_{opt}\left(\%\right) = \frac{Q_{abs}}{A_0 \times I_{dir}} = \rho_0 \times \alpha_0 \times \gamma \times K \tag{18}$$

2.4   THERMAL MODEL

The thermal model based on heat collection element consists of three main components: a stainless steel absorber tube with selective surface surrounded by a partially anti-reflective evacuated glass envelope tube to significantly reduce heat losses and a heat transfer fluid which passes through the absorber tube. When the direct solar radiation is reflected on the heat collection element, most of his energy is absorbed by the glass envelope and the absorber tube surface. The useful heat received from the direct solar radiation is directly transmitted to the heat transfer fluid which enters into the absorber tube with a specific temperature, pressure and mass flow rate and exits it with a pressure and temperature according the boundary conditions found along the heat collection element. In fact, the heat transfer model is based on an energy balance

between the heat transfer fluid and the surroundings. A part of energy absorbed into the absorber is transferred to the heat transfer fluid by forced convection and remaining energy is transferred back to the glass envelope by radiation and natural convection and lost through the support brackets by conduction as well. The heat loss coming from the absorber (radiation and natural convection) passes through the glass envelope by conduction and along with the energy absorbed by the glass envelope is lost to the environment by convection and to sky by radiation.

We have divided the heat collection element into several layers in axial direction and discretized it by using the fully Finite Volume Method and applied an energy balance for each control volume which leads to three partial differential equations of three temperatures solved by using the Tri-Diagonal Matrix Algorithm.
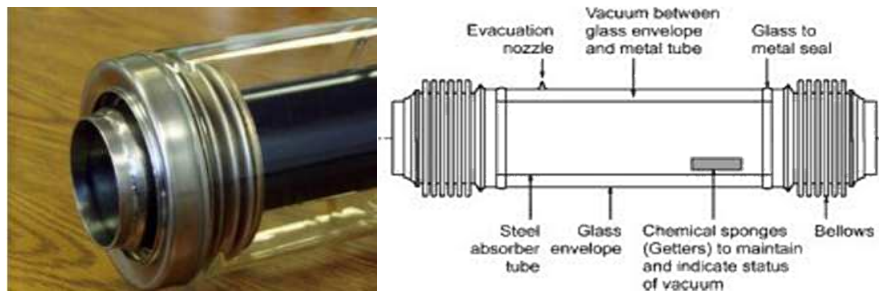
Fig. 1.   Heat collection element, Adapted from [9]
Useful absorptivity (95%) and useful emissivity (14%) with about 350°C and 400°C supported

2.4.1   HEAT BALANCE ON HEAT COLLECTING ELEMENT

By considering a control volume of the heat collection element, the heat balance which leads of three partial differential equations of temperatures of each component of the heat collection element has been expressed as follow:

On the glass envelope, the heat balance is expressed as follows:

$$\underbrace{\rho_{ge}Cp_{ge}A_{ge}\frac{\partial T_{ge}(x,t)}{\partial t}}_{\text{increase internal energy}} = \underbrace{A_0 \times I_{dir} \times \rho_0 \times \alpha_{ge} \times \gamma \times K}_{\text{absorbed solar energy}} + \underbrace{\pi \times d_{eabs} \times h_{c(int)} \times \left(T_{abs} - T_{ge}\right)}_{\text{internal loss}} + \underbrace{A_{ge}k_{ge}\frac{\partial^2 T_{ge}(x,t)}{\partial x^2}}_{\text{thermal diffusion}}$$
$$\underbrace{- \pi \times d_{ege} \times \left[h_{c(ext)} \times \left(T_{ge} - T_{amb}\right) + h_{r(ext)} \times \left(T_{ge} - T_{sky}\right)\right]}_{\text{external loss}}$$

(19)

The cross sectional area of the glass envelope is given as follow:

$$A_{ge}\ (m^2) = \frac{\pi}{4} \times \left(d_{ege}^2 - d_{ige}^2\right)$$

(20)

On the absorber tube, the heat balance is as follows:

$$\underbrace{\rho_{abs}Cp_{abs}A_{abs}\frac{\partial T_{abs}(x,t)}{\partial t}}_{\text{increase internal energy}} = \underbrace{A_0 \times I_d \times \rho_0 \times \alpha_0 \times \gamma \times K}_{\text{absorbed solar energy}} + \underbrace{A_{abs}k_{abs}\frac{\partial^2 T_{abs}(x,t)}{\partial x^2}}_{\text{thermal diffusion}} - \underbrace{\pi \times d_{eabs} \times h_{c(int)} \times \left(T_{abs} - T_{ge}\right)}_{\text{internal loss}}$$
$$- \underbrace{\pi \times d_{iabs} \times h_{u,f} \times \left(T_{abs} - T_f\right)}_{\text{useful heat}}$$

(21)

The cross sectional area of absorber tube is given as follow:

$$A_{abs}\ (m^2) = \pi \times \left(\frac{d_{eabs}^2 - d_{iabs}^2}{4}\right)$$

(22)

On the heat transfer fluid, the heat balance is expressed as follow:

$$\underbrace{\rho_f Cp_f A_f \frac{\partial T_f(x,t)}{\partial t}}_{\text{increase internal energy}} = \underbrace{-Cp_f \frac{\dot{m}_f}{n_{coll}} \frac{\partial T_f(x,t)}{\partial x}}_{\substack{\text{heat converted by} \\ \text{fluid motion}}} + \underbrace{A_f k_f \frac{\partial^2 T_f(x,t)}{\partial x^2}}_{\text{thermal diffusion}} + \underbrace{\pi \times d_{iabs} \times h_{u,f}\left(T_{abs} - T_f\right)}_{\text{useful heat}} \qquad (23)$$

The cross sectional area of heat transfer fluid is given as follow:

$$A_f \ (m^2) = \pi \times \frac{d_{iabs}^2}{4} \qquad (24)$$

2.4.2   ESTIMATION OF EXTERNAL AND INTERNAL HEAT TRANSFER COEFFICIENT

We have considered a heat collecting element with annulus vacuum between the glass envelope and the absorber tube. According to [11], the internal heat transfer coefficient depends on the annulus pressure. When the annulus pressure is less than 13.10^{-3} Pa, the heat transfer coefficient is turn off zero. When the annulus pressure is upper than 13.10^{-3} Pa, the annulus pressure is estimated through natural convection relations between two horizontal concentric cylinders [12], [13].

2.4.2.1   INTERNAL AND EXTERNAL HEAT TRANSFER COEFFICIENT FROM CONVECTION

When the vacuum is turn off zero, natural convection within the annulus occurs. The heat transfer coefficient is then expressed with the Raithby and Holland's correlation [14] for natural convection in an annular space between horizontal cylinders as follow:

$$h_{c(int)}\left(W/m^2\right) = \frac{2 \times k_{eff}}{d_{eabs} \times \ln\left(\frac{d_{ige}}{d_{eabs}}\right)} \qquad (25)$$

The effective thermal conductivity function of the thermo-physical properties of the gas is calculated as:

$$k_{eff} = 0.386 \times k \times \left(\frac{Pr}{0.861 + Pr}\right)^{1/4} \times Ra_c^{1/4} \qquad (26)$$

The equivalent Rayleigh number calculated in equation (28) is used for the range of $(10^2 \le Ra_c \le 10^7)$ and depends on the effective Rayleigh number Ra_{eff} (evaluated at the air gap distance) which also depends on the dimensionless numbers of Grashof and Prandtl as:

$$Ra_c = \frac{\left(\ln\left(\frac{d_{ige}}{d_{eabs}}\right)\right)^4}{L_{eff}^3 \times \left(d_{eabs}^{-3/5} + d_{ige}^{-3/5}\right)^5} \times Ra_{eff} \qquad (27)$$

The air gap distance between the internal diameter of the glass envelope and the external diameter of the absorber tube is calculated as follow:

$$L_{eff} = 0.5\left(d_{ige} - d_{eabs}\right) \qquad (28)$$

The physical properties of the air in annulus vacuums have been calculated at the mean temperature between the absorber tube and the glass envelope as follows:

$$T_{m(air)} = 0.5 \times \left(T_{abs} + T_{ge}\right) \qquad (29)$$

The convection heat transfer coefficient between glass envelope and exterior air is natural in the absence of wind. Thus, for natural convection the correlation developed by Churchill and Chu [15] for horizontal cylinders for the calculation Nusselt number is recommended.

$$h_{c(ext)}\left(W/m^2\right) = \left[0.60 + 0.387 \left(\frac{Ra}{\left(1+\left(\frac{0.559}{Pr}\right)^{\frac{9}{16}}\right)} \right)^{\frac{1}{6}} \right]^2 \frac{k_{air}}{d_{ege}} \tag{30}$$

The physical properties of the exterior air are calculated at the mean temperatures between the glass envelop and the absorber tube as follows:

$$T_{m(ext)} = 0.5 \times \left(T_{abs} + T_{ge}\right) \tag{31}$$

In the presence of wind, the convection heat transfer between glass envelope and exterior air becomes forced and Zhukauskas correlation in equation (36) is recommended:

$$h_{c(ext)}\left(W/m^2\right) = C \times Re^m \times Pr^n \times \left(\frac{Pr}{Pr_{ge}}\right)^{0,25} \times \frac{k_{air}}{d_{ege}} \tag{32}$$

According to [1], the following assumption has been made:

C	m	Re	n	Pr
0.75	0.4	1-40	0.37	<=10
0.51	0.5	$40-10^3$	0.36	>10
0.26	0.6	$10^3-2.10^5$		
0.076	0.7	2.10^5-10^6		

The physical properties of the exterior air are calculated at the ambient temperature while Pr_{ge} is evaluated considering glass envelope temperature.

2.4.2.2   INTERNAL AND EXTERNAL HEAT TRANSFER COEFFICIENT FROM RADIATION

The glass envelope is assumed to be a small convex grey object in a large black body cavity (the sky). By applying the net radiation method, the radiation between the glass envelope and the sky is written as:

$$h_{r(ext)}\left(W/m^2\right) = \sigma \times \varepsilon_{ge} \times \left[\left(T_{e,ge}+273\right)^2 + \left(T_{sky}+273\right)^4 \right]\left(T_{e,ge}+T_{sky}+546\right) \tag{33}$$

The surfaces have been considered as gray and diffuse emitters, absorbers and reflectors. The glass envelope is assumed to be opaque to the infrared radiation. For simplicity and according to the spatial discretization, the radiation in the jth control volume can be approximated as follow:

$$h_{r(int)}\left(W/m^2\right) = \varepsilon_{int} \times \sigma \times \left(\left(T_{abs}+273\right)^2 + \left(T_{ge}+273\right)^2\right) \times \left(T_{abs}+T_{ge}+546\right) \tag{34}$$

Where ε_{int} is calculated in equation (39) with ε_{abs} the emittance of the absorber tube and ε_{ge} the emittance of the glass envelope

$$\varepsilon_{int} = \left(\frac{\frac{d_{ige}}{d_{eabs}}}{\left(\frac{1}{\varepsilon_{abs}}+\frac{1-\varepsilon_{ge}}{\varepsilon_{ge}}\right)} \right) \tag{35}$$

The internal heat transfer flux from convection and radiation is calculated as:

$$Q_{int}\left(W\right) = A_{eabs} \times \left(h_{c(int)}+h_{r(int)}\right) \times \left(T_{abs}-T_f\right) \tag{36}$$

The external heat transfer flux from convection and radiation is calculated as:

$$Q_{ext}(W) = Q_{c(ext)} + Q_{r(ext)} = A_{ge}\left(h_{c(ext)}\left(T_{ge} - T_{amb}\right) + h_{r(ext)}\left(T_{ge} - T_{sky}\right)\right) \tag{37}$$

2.4.2.3 USEFUL HEAT TRANSFER COEFFICIENT

The useful heat transfer coefficient for the convective heat transfer for the heat transfer fluid is calculated as follow:

$$h_{u,f}\left(W/m^2\right) = \frac{Nu_f k_f}{d_{iabs}} \tag{38}$$

To evaluated the useful heat transfer coefficient it is recommend to use Gnielinski [16] correlations' in aim to calculate the Nusselt number in the case of laminar or turbulent flow case and even in the transition region between the laminar and turbulent regime.

For laminar flow at lower Reynolds numbers (Re<2300), the Nusselt numbers Nu_{f1} with constant wall temperature boundary condition and Nu_{f2} with constant heat flux boundary condition are given:

$$Nu_{f1} = \left\{(3,66)^3 + (0,7)^3 + \left(1,615 \times \sqrt[3]{Re_f \times Pr_f \times d} - 0,7\right)^3 + \left(\left(\frac{2}{1+22Pr_f}\right)^{\frac{1}{6}}\sqrt{Re_f \times Pr_f \times d}\right)^3\right\}^{\frac{1}{3}} \tag{39}$$

$$Nu_{f2} = \left\{(4,354)^3 + (0,6)^3 + \left(1,953 \times \sqrt[3]{Re_f \times Pr_f \times d} - 0,6\right)^3 + \left(0,924 \times \sqrt[3]{Pr_f} \times \sqrt{Re_f \times Pr_f \times d}\right)^3\right\}^{\frac{1}{3}} \tag{40}$$

With:

$$d(m) = \frac{d_{iabs}}{L} \tag{41}$$

For turbulent flow at higher Reynolds numbers (Re >4000), the Nusselt number is calculated as:

$$Nu_f = \frac{\frac{f}{8}(Re_f - 1000)Pr_f}{1 + 12.27\left(\frac{f}{8}\right)^{\frac{1}{2}}\left(Pr_f^{\frac{2}{3}} - 1\right)}\left(1 + \left(\frac{d}{L}\right)^{\frac{2}{3}}\right)k_f \tag{42}$$

Where $k_f = \left(\frac{Pr_f}{Pr_{abs}}\right)^{0.11}$ is for liquid and $k_f = \left(\frac{T_f}{T_{abs}}\right)^n$ is for gases and n depend on the gas and it is assumed to be equal to 0.45 for air, in the case of this study.

In equation (42), the friction factor for turbulent flow according to Gnielinski in absorber tube is evaluated as follow:

$$f = \left(1.8 \times \log_{10}\left(Re_{diabs}\right) - 1.5\right)^{-2} \tag{43}$$

In the case of higher values of Pr_f and d , the following friction factor is calculated as:

$$f = \left(1.82 \times \log_{10}\left(Re_{diabs}\right) - 1.64\right)^{-2} \tag{44}$$

For transition region $\left(2300 \leq Re \leq 4000\right)$, Gnielinski proposed equation (45) to estimate the Nusselt number:

$$Nu_f = (1-\chi)Nu_{lam} + \chi Nu_{Tur} \tag{45}$$

With: $\chi = \frac{Re_f}{1700} - \frac{23}{17}$ \tag{46}

The physical properties of the heat transfer fluid are calculated at fluid temperature while Pr_{abs} is evaluated considering absorber temperature.

The global thermal efficiency is defined as follow:

$$\eta_{ther} = \frac{\pi \times d_{iabs} \times h_{u,f} \times (T_{abs} - T_f)}{A_0 \times I_{dir}} \tag{47}$$

2.5 Solution procedure

Finite volume numerical method based on one-dimensional flow has been used to solve this problem. The heat collection element has been divided into three layers in axial direction with energy balance in each control volume. This leads to three algebraic equations (19), (20), (21) which were simultaneously solved by applying the Tri-Diagonal Matrix Algorithm after discretization. Then, the solution obtained based temperature of each component of the heat collection element is as follow:

For glass envelope, $j = 2,P$

$$a_{ge,j}T_{ge,j} = a_{ge,j+1}T_{ge,j+1} + a_{ge,j-1}T_{ge,j-1} + b_{ge} \tag{48}$$

$$a^0_{ge,j} = \varphi_{ge}Cp_{ge}\frac{\Delta x}{\Delta t} \tag{49}$$

$$a_{ge,j} = a^0_{ge,j} + a_{ge,j+1} + a_{ge,j-1} + \pi\frac{\Delta x}{A_{ge}}\left(d_{eabs}h_{(int)} + d_{ege}\left(h_{c(ext)} + h_{r(ext)}\right)\right) \tag{50}$$

$$a_{ge,j+1} = \frac{k_{ge}}{\delta x_{ge,j+0.5}} \tag{51}$$

$$a_{ge,j-1} = \frac{k_{ge}}{\delta x_{ge,j-0.5}} \tag{52}$$

$$b_{ge} = \frac{\Delta x}{A_{ge}}\left[A_0 \times I_{dir} \times \rho_0 \times \alpha_{ge} \times \gamma \times K + \pi\left(d_{eabs}h_{(int)}T_{abs,j+(P+1)} + d_{ev}\left(h_{c(ext)}T_{amb} + h_{r(ext)}T_{sky}\right)\right)\right]a^0_{ge,j}T^0_{ge,j} \tag{53}$$

For absorber tube, $j = P+3, 2P+1$

$$a_{abs,j}T_{g,j} = a_{abs,j+1}T_{abs,j+1} + a_{abs,j-1}T_{abs,j-1} + b_{abs} \tag{54}$$

$$a^0_{abs,j} = \varphi_{abs}Cp_{abs}\frac{\Delta x}{\Delta t} \tag{55}$$

$$a_{abs,j} = a^0_{abs,j} + a_{abs,j+1} + a_{abs,j-1} + \pi\frac{\Delta x}{A_{abs}}\left(d_{eabs}h_{(int)} + d_{iabs}h_{uf}\right) \tag{56}$$

$$a_{abs,j+1} = \frac{k_{abs}}{\delta x_{abs,j+0.5}} \tag{57}$$

$$a_{abs,j-1} = \frac{k_{abs}}{\delta x_{abs,j-0.5}} \tag{58}$$

$$b_{abs} = \frac{\Delta x}{A_{abs}}\left[A_0 \times I_{dir} \times \rho_0 \times \alpha_0 \times \gamma \times K + \pi\left(d_{eabs}h_{(int)}T_{g,j-(P+1)} + d_{iabs}h_{uf}T_{f,j+(P+1)}\right)\right]a^0_{abs,j}T^0_j \tag{59}$$

For heat transfer fluid, $j = 2P+4, 3P+2$

$$a_{f,j}T_{f,j} = a_{f,j+1}T_{f,j+1} + a_{f,j-1}T_{f,j-1} + b_f \tag{60}$$

$$a^0_{f,j} = \frac{\Delta x}{\Delta t}\left(\varphi_f Cp_f\right)^{t+\Delta t} \tag{61}$$

$$a_{abs,j+1} = \frac{k_{f,j+0.5}}{\delta x_{f,j+0.5}} \tag{62}$$

$$a_{f,j-1} = \frac{k_{f,j-0.5}}{\delta x_{f,j-0.5}} + \frac{\dot{m}_f}{A_f} Cp_{f,j-0.5} \tag{62}$$

$$a_{f,j} = \frac{k_{f,j+0.5}}{\delta x_{f,j+0.5}} + \frac{k_{f,j-0.5}}{\delta x_{f,j-0.5}} + \frac{\dot{m}_f}{A_f} Cp_{f,j-0.5} + \frac{\Delta x}{\Delta t}\left(\varphi_f Cp_f\right)^{t+\Delta t} + \pi \frac{\Delta x}{A_f} d_{iabs} h_{u,f} \tag{64}$$

$$b_f = \frac{\Delta x}{A_f}\left[\pi\left(d_{iabs} h_{uf} T_{abs,j-(P+1)}\right)\right] a^0_{f,j} T^0_{f,j} \tag{65}$$

By considering that external node corresponds to boundary node for each sub-system, we have assumed the boundary conditions as follow:

- outer of glass envelope: adiabatic boundary conditions on both inlet and outlet surfaces;
- absorber tube: adiabatic boundary conditions on inlet and outlet surfaces;
- heat transfer fluid: uniform inlet temperature and adiabatic boundary assumption on outlet temperature.

Then, we have at all:

For j=1

$$a_{ge,2} = 1 \quad a_{ge,-1} = 0 \quad a_{ge,1} = 1 \quad b_{ge} = 0 \tag{66}$$

For j=P+1

$$a_{ge,P+2} = 0 \quad a_{ge,P} = 1 \quad a_{ge,P+1} = 1 \quad b_{ge} = 0 \tag{67}$$

For j=P+2

$$a_{abs,P+3} = 1 \quad a_{abs,P+1} = 0 \quad a_{abs,P+2} = 1 \quad b_{abs} = 0 \tag{68}$$

For j=2P+2

$$a_{abs,2P+3} = 0 \quad a_{abs,2P+1} = 1 \quad a_{abs,2P+2} = 1 \quad b_{abs} = 0 \tag{69}$$

For j=2P+3

$$a_{f,2P+4} = 1 \quad a_{f,2P+2} = 0 \quad a_{f,2P+3} = 1 \quad b_f = T_e \tag{70}$$

For j=3P+3

$$a_{f,3P+4} = 0 \quad a_{f,3P+2} = 1 \quad a_{f,3P+3} = 1 \quad b_f = 0 \tag{71}$$

The algebraic system of three equations were solved simultaneously by using the direct method of Tri-Diagonal Matrix Algorithm, with a temperature tolerance of 10^{-2} and time step $\Delta t = 10s$ and inter nodal distance $\Delta x = 0.2m$ are optimized to get a good convergence with small computational cost. The initial value of the temperature is assumed to be equal to the ambient temperature.

3   RESULTS AND DISCUSSION

Programing equation of a solar parabolic trough collector was performed in this work. Finite volume method based on one-dimensional flow was devoted to discretize three partial differential equations from the model and implemented by using Tri-Diagonal Matrix Algorithm. In order to validate the solar radiation model, solar radiation components' estimated were compared with measurements campaigns from weather station of Maroua Sallack Airport. Also, thermal model was validated by comparing results from Sandia experimental tested collector and results from other devoted works. Results

were displayed by considerate two seasons: then months of hot and dry season characterized by sunny months and two months of wet seasons characterized by less sunny months. A typical day of both the sunniest and the least sunny months of those seasons lead to useful results.

3.1 SOLAR RADIATION COMPONENT'S ESTIMATED

In figure 2, direct, diffuse and global solar radiations estimated on a horizontal plane in Maroua are presented. The solar radiation model, implemented by using the empirical model of Capderou based clear skies is compared with measurements campaigns from the weather station of Maroua Sallak Airport. The figure shows that the empirical model of Capderou gives acceptable estimate of direct, diffuse and global solar radiation during a typical day of the least sunny month of wet season in Maroua.
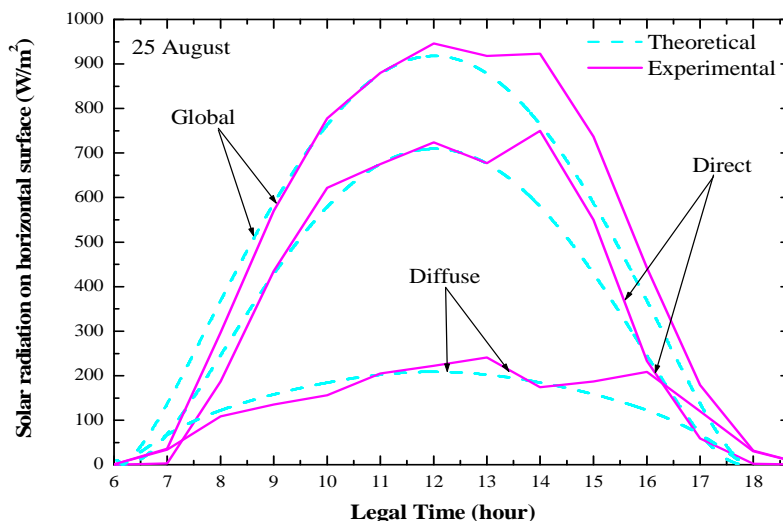
Fig. 2. Direct, diffuse and global solar radiation validated with measurements campaigns from Maroua Sallak Airport during a typical day of the least sunny month

According to figure 3, the direct solar radiation estimated during a typical day of the least sunny month is about 800W/m^2 with full tracking mode. In addition, compared to the E-W horizontal tracking mode which gives good estimation than the E-W polar tracking mode in the same climatic conditions, the full tracking mode is more suitable than the others mode because of maximum amount of energies absorbed while the N-S horizontal mode consumes less energy compared to the others mode.
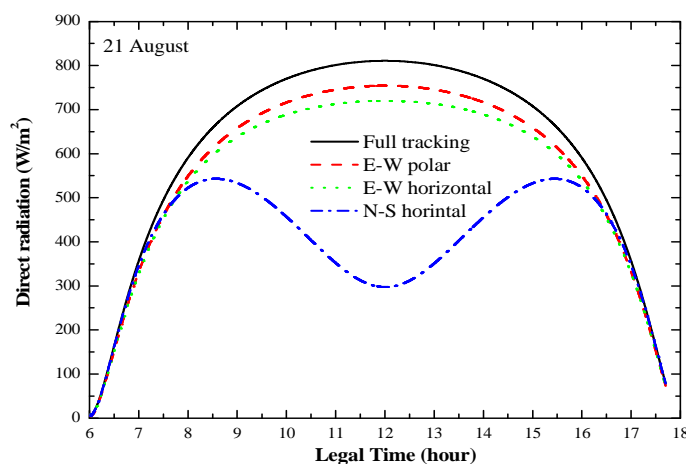
Fig. 3. Direct solar radiation on a horizontal plane for various tracking mode during a typical day of the least sunny month

3.2 OPTICAL PERFORMANCES

The optical efficiency for various tracking mode is displayed during a typical day of the sunniest month (Figure 4). It is observed that, the full tracking mode collectes the maximum amount of energy with about 74% of optical eficiency. In addition, the optical performances from E-W horizontal and E-W polar mode is getting closer with full tracking mode for both the sunny and the less sunny months.
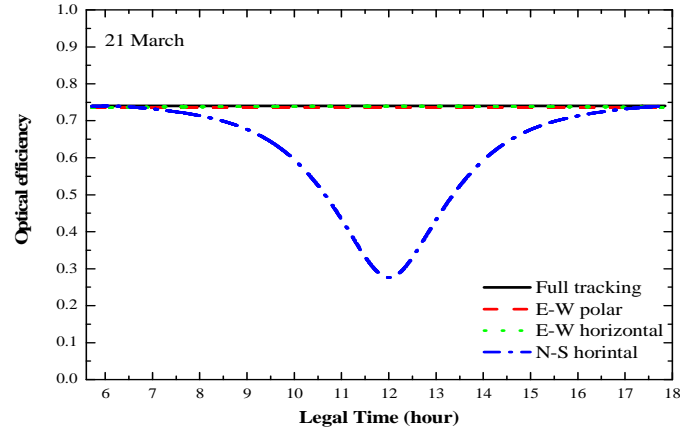
Fig. 4.   *optical efficiency for various tracking mode on a typical day of the sunniest month*

The daily annual average of optical efficiency is displayed (Figure 5) for various tracking modes. This result shows that, the E-W polar and the E-W horizontal modes are better for solar parabolic trough collectors. In these conditions, if we consider a solar parabolic trough collector field with several collectors, the E-W horizontal tracking mode is better due to the low power losses by field's shadow. In another hand, the E-W polar solar tracking system is preferred for individual installation because of the small surface of the reflector.
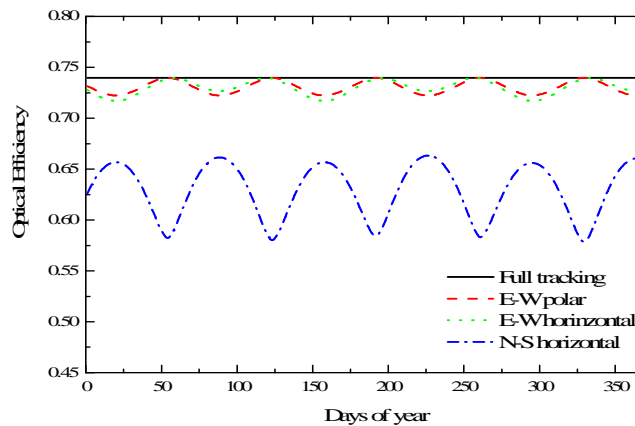
Fig. 5.   *Daily annual average of optical efficiency for various tracking modes*

3.3 THERMAL PERFORMANCES

The thermal performances of the model are estimated under the same climatic conditions during a typical day of the sunniest and the least sunny months for air, water and TherminolVP-1^{TM} synthetic oil. The inlet temperature assumes is at about 25°C; with wind speed at around 2m/s and mass flow rate equal to 0.08kg/s. The flow rate has been supposed to be turbulent and the East-West horizontal solar tracking mode which is getting closer with full tracking is assumed to be in high optical efficiency at about 74% during all the seasons. The model is validated by comparing results from Sandia experimental tested parabolic trough collector and results from another devoted work.

Table 4.   Comparison of the outlet temperature between Sandia experimental tested parabolic trough collector and simulation results.

Fluid	I_{dir} (W/m^2)	m_f (l/min)	T_{inlt} (°C)	Exp ΔT(°C)	Ref [17] ΔT(°C)	Model ΔT(°C)	Error (%) Exp Vs Ref [29]	Error (%) Exp Vs Model
Water	807.9	18.4	18.3	17.8	17.79	17.8	0.056	0.00
Syltherm 800	933.7	47.7	102.2	21.8	21.25	21.78	2.52	0.092

In figure 6, temperatures variation at the output of absorber tube and glass envelope are displayed during a typical day of the sunniest months by using air, water and TherminolVP-1^{TM} as heat transfer fluids.
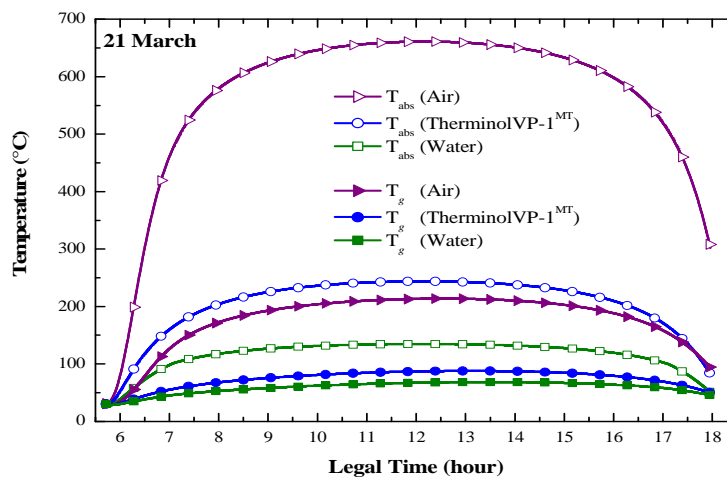
Fig. 6.   Output temperature of the absorber tube and glass envelope for a typical day of the sunniest month

Temperatures variation at the output of absorber tube and glass envelope are displayed (Figure 7) during a typical day of the least sunny month by using air, water and TherminolVP-1^{TM} as heat transfer fluids.
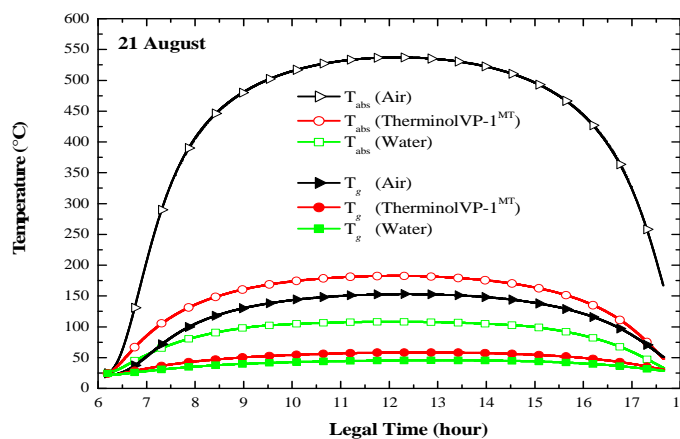
Fig. 7.   Output temperature of the absorber and glass envelope for a typical day of the sunny month

Figure 8 display the temperature variation along the absorber tube for three different heat transfer fluids during a typical day of the sunniest month. It is observed that, oil and air temperatures increase much faster compared to water temperature.
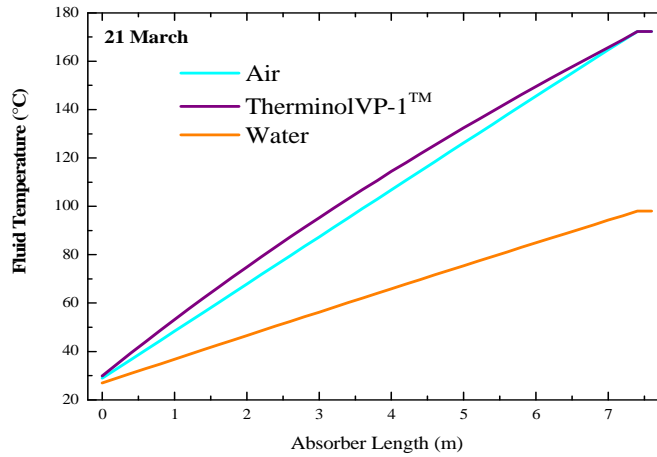
Fig. 8.   Fluid temperature variation along the absorber tube assumed at 13h during a typical day of the sunniest month

During a typical day of the least sunny month, the maximum of outlet temperature of heat transfer fluid obtained at the right end of the absorber tube is about 140°C, 138°C and 80°C for air, synthetic oil and water respectively (Figure 9).
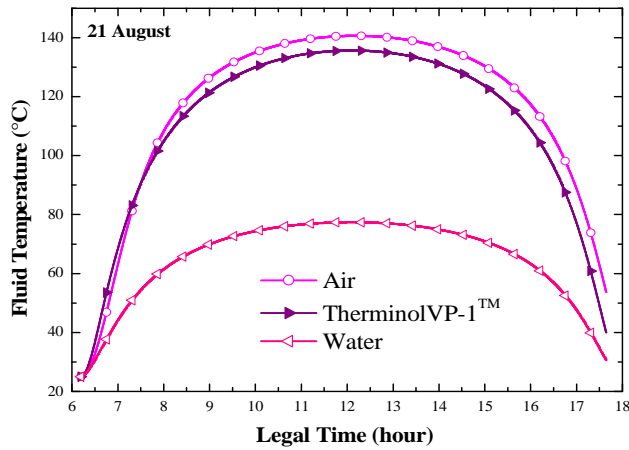
Fig. 9.   Outlet temperature of the heat transfer fluid during a typical day of the least sunny month

During a typical day of the sunniest month, the maximum of outlet temperature of heat transfer fluid obtained at the right end of the absorber tube is about 180°C for both air and oil and 90°C for water (Figure 10).
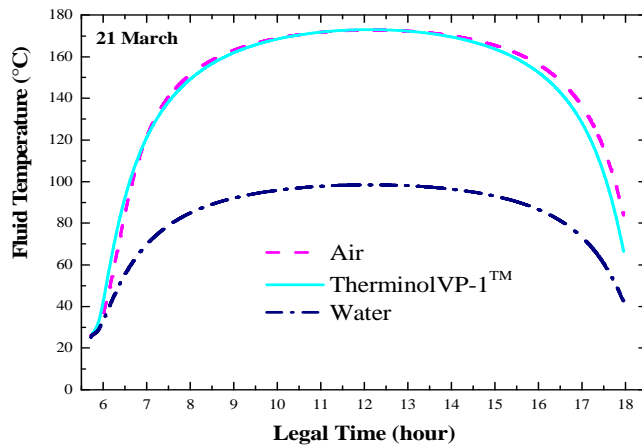
Fig. 10.   Outlet temperature of the heat transfer fluid for a typical day of the sunny months

The heat gained depends on the type of heat transfer fluid. For a typical day of the sunniest month, the much maximum of heat gained is reached in the mid-day and it is from TherminolVP^{TM} with about 78kW, 45kW and 20kW for TherminolVP^{TM}, water and air respectively (Figure 11).
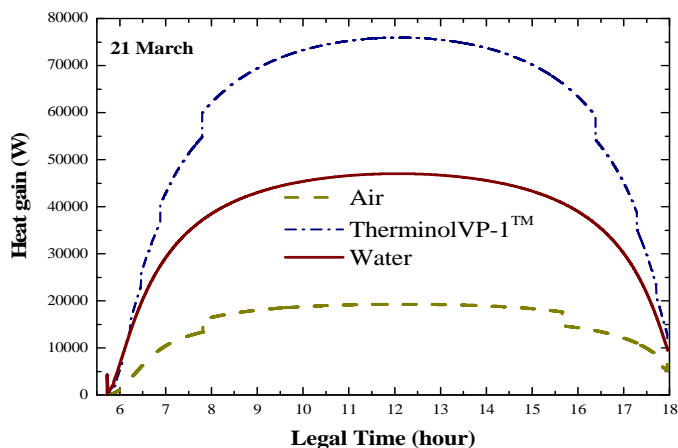
Fig. 11. Useful heat gained during a typical day of the sunniest month

It can be observed that, the heat loss follows perfectly the temperature profile of the absorber. Then, the thermal oil (TherminolVP^{TM}) considered in this study is not only highly stable but also designed for high temperature liquid phase operation with good heat transport and transfer properties (Figure 12).
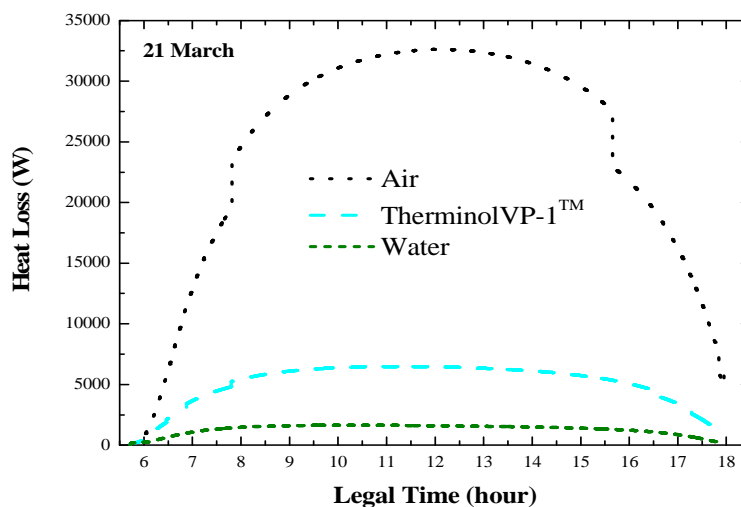
Fig. 12. Heat loss during a typical of the sunniest month

4   CONCLUSION

Optical and thermal performances of a solar parabolic trough collector with water, air or TherminolVP-1^{TM} synthetic oil used as heat transfer fluid under climatic conditions of Cameroon Sahelian Zones have been developed throughout this work. The empirical model of Capderou has been used to model direct solar radiation and solar energy absorbed by the collector in Far North Region of Cameroon. Results of solar radiation components obtained were compared with measurements campaigns from the weather station of Maroua Sallak Airport. The thermal model based on an energy balance has led to three partial differential equations of temperatures discretized by applying the fully Finite Volume Method and solved by implementing the Tri-Diagonal Matrix Algorithm. A computer program has led to estimate optical efficiency of the collector which reached at about 74% with full tracking mode during all the seasons. In addition, in aim to reduce the cost of the system, East-West Horizontal and East-West polar solar tracking are suitable. Moreover, outlet temperatures of heat transfer

fluids obtained were compared with data from Sandia experimental tested collector and from another devoted work. According to the results obtained, it can be concluded that the current numerical model is suitable for predicting the optical and thermal behaviors of a solar parabolic trough collector under operating conditions of Cameroon Sahelian Zones. For low temperature applications (T<180°C) such as domestic heat water, refrigeration, distillation, industrial process heat and air conditioning, water as heat transfer fluid is more suitable due to its low cost and good thermal performances to use while air and synthetic oil are better for very high temperature applications such as electricity production. Cameroon Sahelian Zones is a huge reservoir of solar energy and water resources from rivers and many Lakes and those potential could be exploited for small needs in the case of low temperature applications.

Further work is ongoing for determining the predictive model control of a solar parabolic trough collector under climatic conditions of Far North Cameroon Region. It is also very interesting to conduct the same study in regards of solar photovoltaic systems. This will lead to compare solar parabolic trough collector with solar photovoltaic systems performances under climatic conditions of Sahelian zones.

REFERENCES

[1] Kalogirou Soteris A., ''A detailed thermal model of a parabolic trough collector receiver,'' Energy (2012) 48 (1) pp. 298-306.

[2] Ya-Ling. He, Jie. Xiao, Ze-Dong. Cheng, Yu-Bing. Tao, ''A MCRT and FVM coupled simulation method for energy conversion process in parabolic trough solar collector,'' Renewable Energy 36 (2011) pp. 976-985.

[3] Dudley, V. E., Kolb, G. J., Sloan, M., Kearney, D et al., 1994. "Test Results: SEGS LS 2 Solar Collector". SAND94-1884. Albuquerque, NM: SANDIA National Laboratories.

[4] A.A. Hachicha, I. Rodríguez, R. Capdevila and A. Oliva, ''Heat transfer analysis and numerical simulation of a parabolic trough solar collector,'' Applied Energy 2013; 111: 582-592.

[5] Ouagued M, Khellaf A, Loukarfi L, ''Estimation of the temperature, heat gain and heat loss by solar parabolic trough collector under Algerian climate using different thermal oils,'' Energy Conversion and Management 75 (2013) pp. 191-201.

[6] Mohanad Abdulazeez Abdulraheem Alfellag, ''Modeling and Experimental Investigation of Parabolic Trough Solar Collector,'' Embry-Riddle Aeronautical University-Daytona Beach, pp. 95, 2014.

[7] Yacine Marif, Hocine Benmoussa, Hamza Bouguettaia, Mohamed M. Belhadj, Moussa Zerrouki, ''Numerical simulation of solar parabolic trough collector performance in the Algeria Saharan region.'' Energy Conversion and Management 85 (2014) pp. 521-529.

[8] Joseph Kessel Pombe, Camelia Stanciu, Haman-Djalo, Viorel Badescu, Beda Tibi, ''Modélisation thermodynamique d'un récepteur tubulaire pour concentrateurs solaires de type linéaire,'' International Journal of Scientific Research & Engineering Technology (IJSET), Vol. 3, pp. 19-26, 2015.

[9] Dudley V, Kolb G, Sloan M, Kearney D, ''SEGS LS2 solar collector-test results,'' Tech. Rep.; Report of Sandia National Laboratories (SANDIA-94-1884); 1994.

[10] Capderou M., ''Atlas Solaire de l'Algérie, Modèles Théoriques et Expérimentaux,'' Volume1, Tome 2, Office des Publications Universitaires, Algérie 1987.

[11] R. Capdevila, O. Lehmkuhl, C.D. Pérez-Segarra, G. Colomer, ''Turbulent natural convection in a differentially heated cavity of aspect ratio 5 filled with non-participating and participating grey media,'' International Journal of physics: conference series, 2011. Doi: 10.1088/1742-6596/318/4/042048.

[12] M. M. Zdravkovich, ''Flow around circular cylinders,'' volume 2. Oxford University Press, 2003.

[13] Padilla Ricardo. V, Demirkaya. G, Goswami. D. Yogi, Stefanakos. E, Muhammad M. Rahman, ''Heat transfer analysis of parabolic trough solar receiver,'' Applied Energy 88 (2011), pp. 5097-5110.

[14] Raithby GD, Hollands K., ''A general method of obtaining approximate solutions to laminar and turbulent free convection problems,'' Advances in Heat Transfer 1975, 11:265-315.

[15] Churchill S, Chu H., ''Correlating equations for laminar and turbulent free convection from a horizontal cylinder,'' Int J Heat Mass Trans 1975, 18(9), 1049-53.

[16] Gnielinski V., ''New equations for heat and mass transfer in turbulent pipe and channel flow,'' International Chemical Engineering 1976, 16(2), 359-63.

[17] O. Garcia-Valladares and N. Velazquez, ''Numerical simulation of parabolic trough collector: improvement using counter flow concentric circular heat exchangers,'' International journal of heat and mass transfer, Vol. 52 (3-4), 597-609 (2009).